Proceedings of the 1998 IEEE/RSJ
Intl. Conference on Intelligent Robots and Systems
Victoria, B.C., Canada • October 1998

Kinematic/Dynamic Analysis of a 6 DOF Parallel Manipulator with 3-PPSP Serial Subchains and its Implementation

Yong-kyu Byun*, Hyung-suck Cho, Whee-kuk Kim***,**
Sang-eun Baek*, Heung-sung Chang*, Kwang-choon Ro*
* Electromechanics Lab. Samsung Adv. Inst. of Tech., Korea
** Dept. of Mechaincal Eng., KAIST, Korea
*** Dept. of Control & Instrumentation Eng., Korea Univ., Korea

Abstract

In this paper, the kinematic analysis for a 6 degree-of-freedom parallel manipulator with 3-PPSP type serial subchains is performed and its kinematic characteristics are investigated via isotropic index of the first-order kinematic influence matrix. Also, dynamic analysis of the manipulator is performed and its dynamic characteristics is examined via the isotropic characteristics of the output effective inertial matrix. From the analysis results, it can be concluded that the manipulator has an excellant kinematic and dynamic characteristics required for high precision manipulators. Lastly, a prototype manipulator system is implemented and the joint position servo-controller is applied to the system. Noting the manipulator has closed-form forward/reverse position solutions[8], it is expected that more advanced controller requiring heavy computational burden can be applied to the system in real time to further enhance the performane of the system.

I. Introduction

Parallel mechanism has an excellent structure for exerting high precision performance and high stiffness due to its kinematically constrained structure. However, in general, the complexity of its kinematic/dynamic analysis of the parallel mechanism prohibits itself from being applied to various application area. To overcome this problem, various parallel structures and kinematic/dynamic modeling methods have been suggested in literature.

Recently, Reboulet[1] studied dynamic model employing the simplified Newton-Euler method which is expressed in terms of differential equations in its movable workspace. Thomas and Tesar[2] proposed the dynamic modeling method for the serial manipulator by introducing the kinematic influence coefficient(KIC) concepts, and Freeman and Tesar[3] extended the modeling method so that it is applicable to parallel manipulators by introducing the method of transfer of coordinate systems. Sklar and Tesar[4] further extended the dynamic modeling method applicable to any hybrid manipulators. These modeling methods[2,3,4] are so systematic that they can be easily applied to parallel manipulators.

Byun[5] proposed the 3-PPSP type 6 degrees-of-freedom parallel mechanism. Later, Kim and Byun[6] suggested the closed-forms of forward and reverse position solutions for the mechanism of general geometry. Noting that when the closed-form solution of kinematic position analysis of the system exists, the computation burden for carrying out its kinematic analysis in real time operation is significantly reduced.

Therefore, in this paper, kinematic and dynamic models of the 3-PPSP 6 degrees-of-freedom mechanism are obtained, using the method of transfer of coordinates system proposed by Freeman and Tesar[3]. Then its kinematic and dynamic characteristics are investigated. Lastly, the prototype of the mechanism is implemented and brief description of the implemented system is discussed. Then, by applying the simple position serve control algorithm, the performance of the implemented manipulator is tested.

2. Description of the 3-PPSP parallel mechanism

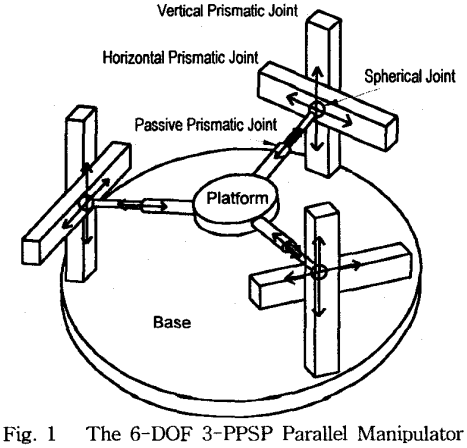

Fig. 1 The 6-DOF 3-PPSP Parallel Manipulator

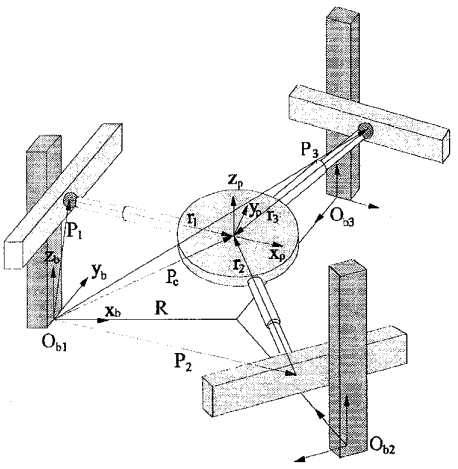

Fig. 2 Kinematic Model

Fig. 1 shows the schematic diagram for the 3-PPSP parallel mechanism. The mechanism consists of a top plate, a base plate and 3-PPSP type serial subchains connecting those two plates. Each of serial subchains is made of two active prismatic joints(PP), one spherical joint(S) and one passive prismatic joint(P). The passive prismatic joints are constrained to move parallel to the top plate. Let's define $(\boldsymbol{x}_b\ \boldsymbol{y}_b, \boldsymbol{z}_b)$ and $(\boldsymbol{x}_p\ \boldsymbol{y}_p\ \boldsymbol{z}_p)$ as the reference frame fixed on the base plate and the output frame fixed to the top plate, respectively, as shown in Fig. 2. And denote $\boldsymbol{P}_c=[P_{cx}\ P_{cy}\ P_{cz}]^T$ as the output position vector from the origin(O_b) of the reference frame to the origin(O_p) of the output frame. The output orientation is expressed using the $x-y-z$ Euler angles as below

$$[R_b^p]=[Rot(\boldsymbol{x},\alpha)][R(\boldsymbol{y},\beta)][Rot(\boldsymbol{z},\gamma)] \quad (1)$$

Then, the input vector and the output vector of the mechanism are defined as

$$\boldsymbol{d}=[\,{}_1d_1\ {}_1d_2\ {}_2d_1\ {}_2d_2\ {}_3d_1\ {}_3d_2]^T \quad (2)$$

and

$$\boldsymbol{E}_o=[P_{cx}\ P_{cy}\ P_{cz}\ \alpha\ \beta\ \gamma]^T, \quad (3)$$

respectively, where ${}_id_j$ represents the j^{th} joint of the i^{th} serial subchain of the mechanism. Also, the position vectors from the origin of the reference frame to the origin(O_{bi}) of the i^{th} local frame are denoted as $\boldsymbol{P}_{bi}$(for $i=1,2,3$) and the rotation matrix from the reference frame to the i^{th} local frame are represented as [${}_iR_b^o$]. Table 1 represents Denavit-Hartenberg link parameters for one of three serial subchains and Fig. 3 illustrates the those link parameters.

3. Kinematic model of a 3-PPSP mechanism

Denote $\boldsymbol{\omega}$ and $\dot{\boldsymbol{\mu}}=[\dot{\alpha}\ \dot{\beta}\ \dot{\gamma}]^T$ as the absolute angular velocity vector and the Euler rate vector of the output frame. Noting that the following relationship holds between the absolute angular velocity and the Euler rate vector,

$$\boldsymbol{\omega}=[R_b^p]\,\dot{\boldsymbol{\mu}}, \quad (4)$$

the output velocity vector is defined as

$$\dot{\boldsymbol{u}}=[\ \dot{\boldsymbol{P}}_c^T\ \ \boldsymbol{\omega}^T]^T \quad (5)$$

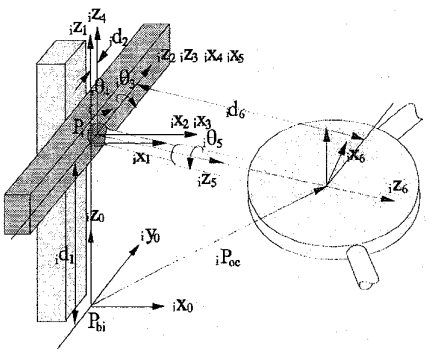

Fig. 3 Kinematic Model of a PPSP Serial Subchain

Table 1 DH link parameter of PPSP serial subchain

Link # n	α_{n-1}	a_{n-1}	d_n	θ_n
1	0	0	d_1	0
2	-90	0	d_2	0
3	0	0	0	θ_3
4	90	0	0	θ_4
5	90	0	0	θ_5
6	0	0	d_6	0
Top plate	-90	0	0	${}_i\gamma_t$

3.1 The first order kinematic model of a serial subchain

3.1.1 rotational first-order KIC

Denote ${}_i\boldsymbol{\omega}_j$ as the absolute angular velocity of the j^{th} link of the i^{th} serial subchain and ${}_i\boldsymbol{v}_j$ as the absolute translational velocity of a point of interest P_j fixed on the same link. They are combined to form a vector ${}_i\dot{\boldsymbol{u}}_j$ representing the output velocity vector of the j^{th} link of the i^{th} serial subchain as below,

$${}_i\dot{\boldsymbol{u}}_j=[\ {}_i\boldsymbol{v}_j^T\ \ {}_i\boldsymbol{\omega}_j^T]^T \quad (6)$$

Let ${}_i\boldsymbol{\phi}=[\,{}_i\phi_1\ {}_i\phi_2\ \cdots\ {}_i\phi_N]^T$ be the joint velocity

vector of the i^{th} serial subchain. Then the relationship between ${}_i\boldsymbol{\omega}_j$ and ${}_i\dot{\boldsymbol{\phi}}$ can be expressed as

$$ {}_i\boldsymbol{\omega}_j = [\ {}_iG_{\phi}^{jk}]\ {}_i\dot{\boldsymbol{\phi}} \tag{7} $$

where $[\ {}_iG_{\phi}^{jk}]$ represents the rotational 1^{st} order KIC.

3.1.2. Translational first-order KIC

The absolute translational vector of an arbitrary point P_j fixed on the j^{th} link of the i^{th} serial subchain, ${}_i\boldsymbol{v}_j$, can be obtained as

$$ {}_i\boldsymbol{v}_j = [\ {}_iG_{\phi}^{P_j}]\ {}_i\dot{\boldsymbol{\phi}} \tag{8} $$

where $[\ {}_iG_{\phi}^{P_j}]$ represents the translational first order KIC for the point P_j. From eq. (7) and (8), the velocity relationship between output vector and input vector can be written as

$$ \dot{\boldsymbol{u}} = [\ {}_iG_{\phi}^{u}]\ {}_i\dot{\boldsymbol{\phi}} \tag{9} $$

where $[\ {}_iG_{\phi}^{u}]$ represents Jacobian (the first order KIC) of the i^{th} serial subchain.

3.2 The first-order KIC of the parallel mechanism

when the Jacobian of each of serial subchain is nonsingular, inverse relationship of eq. (9) is expressed as

$$ {}_i\dot{\boldsymbol{\phi}} = [\ {}_iG_{\phi}^{u}]^{-1}\dot{\boldsymbol{u}}, \quad (\text{for } i=1,2,3) \tag{10} $$

From eq. (10), the relationship between active joint input velocity vector $\dot{\boldsymbol{\phi}}_a\ (=\dot{\boldsymbol{d}})$ and the output velocity vector $\dot{\boldsymbol{u}}$ can be written as

$$ \dot{\boldsymbol{\phi}}_a = [\ G_u^a]\ \dot{\boldsymbol{u}} \tag{11} $$

Finally, the forward kinematic relationship between the output velocity vector and input velocity vector can be found by directly inverting eqn. (11) as follows.

$$ \dot{\boldsymbol{u}} = [\ G_a^u]\ \dot{\boldsymbol{\phi}}_a. \tag{12} $$

3.3 The second-order KIC of serial subchains

3.3.1. Rotational 2^{nd} order kinematic analysis

By differentiating eq. (7) with respect to time, relationship between absolute angular acceleration vector of the j^{th} link of the i^{th} serial subchain and the input joint variable vector can be written as,

$$ \begin{aligned} {}_i\ddot{\boldsymbol{a}}_j &= [\ {}_iG_{\phi}^{jk}]\ {}_i\ddot{\boldsymbol{\phi}} + \left(\frac{d}{dt}[\ {}_iG_{\phi}^{jk}]\right)\ {}_i\dot{\boldsymbol{\phi}} \\ &= [\ {}_iG_{\phi}^{jk}]\ {}_i\ddot{\boldsymbol{\phi}} + {}_i\dot{\boldsymbol{\phi}}^T[\ {}_iH_{\phi\phi}^{jk}]\ {}_i\dot{\boldsymbol{\phi}} \end{aligned} \tag{13} $$

where $[\ {}_iH_{\phi\phi}^{jk}]$ represents the 2^{nd} order KIC of the j^{th} link with respect to input joint variables.

3.3.2 Translational 2^{nd} order kinematic analysis

The relationship between the translational acceleration vector of the point fixed to the j^{th} link of the i^{th} serial subchain and the joint acceleration vector of the i^{th} serial subchain can be obtained by direct differentiation of eq. (10) with respect to time, as follows,

$$ \begin{aligned} {}_i\ddot{\boldsymbol{a}}_j &= [\ {}_iG_{\phi}^{P_j}]\ {}_i\ddot{\boldsymbol{\phi}} + \left(\frac{d}{dt}[\ {}_iG_{\phi}^{P_j}]\right)\ {}_i\dot{\boldsymbol{\phi}} \\ &= [\ {}_iG_{\phi}^{P_j}]\ {}_i\ddot{\boldsymbol{\phi}} + {}_i\dot{\boldsymbol{\phi}}^T[\ {}_iH_{\phi\phi}^{P_j}]\ {}_i\dot{\boldsymbol{\phi}} \end{aligned} \tag{14} $$

where $[\ {}_iH_{\phi\phi}^{P_j}]$ represents the translational 2^{nd} order KIC. Particularly, it can be noted that for the 3-PPSP parallel mechanism the position vectors representing the mass centers of the third and the fourth links can be approximated as

$$ {}_i\boldsymbol{P}_{c3} = {}_i\boldsymbol{R}_3 \tag{15} $$

$$ {}_i\boldsymbol{P}_{c4} = {}_i\boldsymbol{R}_4. \tag{16} $$

From (13) and (14), the relationship between the output acceleration and the input joint vector of the serial subchain is obtained as

$$ \ddot{\boldsymbol{u}} = [\ {}_iG_{\phi}^{u}]\ {}_i\ddot{\boldsymbol{\phi}} + {}_i\dot{\boldsymbol{\phi}}^T[\ {}_iH_{\phi\phi}^{u}]\ {}_i\dot{\boldsymbol{\phi}} \tag{17} $$

where $[\ {}_iH_{\phi\phi}^{u}]$ represents the 2^{nd} KIC of the j^{th} link of the i^{th} serial subchain with respect to the joints of the i^{th} serial subchain.

The inverse relationship of eq. (17) is written as

$$ {}_i\ddot{\boldsymbol{\phi}} = [\ {}_iG_{\phi}^{u}]^{-1}\ddot{\boldsymbol{u}} + \boldsymbol{u}^T[\ {}^iH_{uu}^{\phi}]\ \dot{\boldsymbol{u}}. \tag{18} $$

From eq. (18), the acceleration relationship between output variables and active input joint variables is expressed as

$$ \ddot{\boldsymbol{\phi}}_a = [\ G_{\phi}^{u}]^{-1}\ddot{\boldsymbol{u}} + \boldsymbol{u}^T[H_{uu}^{a}]\ \dot{\boldsymbol{u}} \tag{19} $$

Finally, the inverse relationship is found as follows

$$ \ddot{\boldsymbol{u}} = [\ G_{\phi}^{u}]\ \ddot{\boldsymbol{\phi}}_a + \boldsymbol{\phi}_a^T[H_{\phi\phi}^{u}]\ \dot{\boldsymbol{\phi}}_a \tag{20} $$

and this is the acceleration relationship between the active joint input vector $\boldsymbol{\phi}_a$ and the output vector $\boldsymbol{u}$.

3.4 Analysis on kinematic characteristics of the mechanism

To investigate kinematic characteristics of the mechanism, kinematic isotropic index defined by

$$ \sigma_{KI} = \frac{\sigma_{\min}([\ G_a^u])}{\sigma_{\max}([\ G_a^u])} \tag{21} $$

is used. In the simulation, it is assumed that two active prismatic joints of each of serial subchains are placed perpendicular to the base and that its motion plane formed by those two active prismatic joints is placed vertically to the base and tangentially to the circle of radius of $R=0.195$ located at the center of the base as shown in Fig. 2. Therefore, those three motion planes meet each other at an angle of 60^o, and the circle of radius of R and the motion planes intersects at three points where the first active joint of each of serial subchains is placed symmetrically with

an angle 120^o each other.

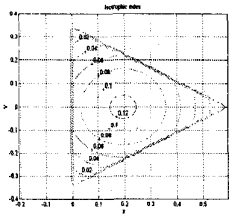

(a) $\alpha=\beta=\gamma=0^o$

$P_{cz}=0,\ \phi_{smax}=90^o$

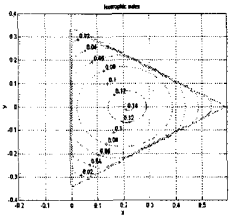

(b) $\alpha=30^o,\ \beta=\gamma=0^o$

$P_{cz}=0,\ \phi_{smax}=90^o$

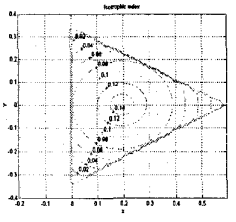

(c) $\alpha=\beta=0^o,\ \gamma=30^o,$

$P_{cz}=0,\ \phi_{smax}=90^o$

Fig. 4 Contour Plots of Isotropic Index in $x-y$ plane

Fig. 4a)-c) represents the contour plot of the isotropic index in the $x-y$ plane when $P_{cz}=0$, $\phi_{smax}=90^o$ and the orientation of the top plate is set to be a) $\alpha=\beta=\gamma=0^o$, b) $\alpha=30^o$, $\beta=\gamma=0^o$, c) $\alpha=\beta=0^o$, $\gamma=30^o$, respectively. It can be confirmed from these plots that the isotropic property of the mechanism is not affected significantly for the variation of the orientation of the top plate. Fig. 5a)-c) represents the contour plot of the isotropic index in the $\alpha-\beta$ plane when $P_{cz}=0$, $\phi_{smax}=90^o$ and the output position and orientation of the top plate is set to be a) $P_{cx}=P_{cy}=0$, $\gamma=0^o$, b) $P_{cx}=0.1$, $P_{cy}=0$, $\gamma=0^o$, c) $P_{cx}=0.1$, $P_{cy}=0$, $\gamma=30^o$.

It can be seen from these plots that the parallel mechanism has the uniform kinematic characteristics around the center of its workspace.

4. Dynamic modeling of the 3-PPSP parallel mechanism

4.1 dynamic modeling of a serial subchain

Denote $[\ {}_i\Pi_{jk}]$ and $[\Pi_{jk}^{(j)}]$ represents the global inertia matrix of the j^{th} link of the i^{th} serial subchain about its mass center and the local inertia matrix with

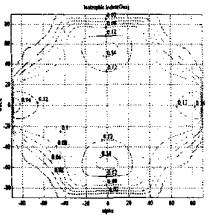

(a) $\phi_{smax}=90^o\ P_{cz}=0$

$P_{cx}=P_{cy}=0,\ \gamma=0^o$

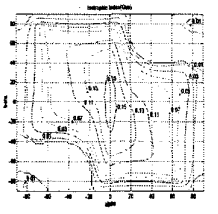

(b) $P_{cx}=0.1, P_{cy}=0, \gamma=0^o$

$P_{cz}=0,\ \phi_{smax}=90^o$

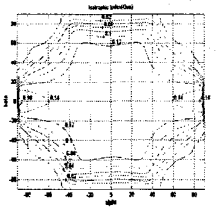

(c) $\gamma=30^o\ P_{cx}=0.1,\ P_{cz}=0$

$P_{cy}=0\ \phi_{smax}=90^o$

Fig. 5 Contour Plots of Isotropic Index in $\alpha-\beta$ plane

respect to the local frame at the center of the j^{th} link, respectively. They are related to each other as below

$$[\ {}_i\Pi_{jk}]=[\ {}_iR_b^j][\ {}_i\Pi_{jk}^{(j)}][\ {}_iR_b^j]^T,\quad j=1,2,\cdots,N \tag{22}$$

Dynamic equation of the i^{th} serial subchain can be expressed as

$$ {}_i\tau_\phi=[\ {}_iI_{\phi\phi}^*]\ {}_i\ddot{\phi}+\ {}_i\phi^T[\ {}_iP_{\phi\phi\phi}^*]\ {}_i\dot{\phi} \tag{23}$$

where $[\ {}_iI_{\phi\phi}^*]$ and $[\ {}_iP_{\phi\phi\phi}^*]$ represents the effective inertia matrix and the effective inertia power array with respect to joint variables, respectively.

4.2 Dynamic model of the parallel mechanism

From the principle of the virtual work, the relationship between joint torques and output torques is expressed as

$$ {}_i\tau_\phi\cdot\ \delta\ {}_i\phi=\tau_u\cdot\ \delta u. \tag{24}$$

Using eq. (9) and eq. (24), the dynamic equation of the i^{th} serial subchain in operational space is written as

$$ {}_i\tau_u=[\ {}_iI_{uu}^*]\ \ddot{u}+\ u^T[\ {}_iP_{uuu}^*]\ \dot{u} \tag{25}$$

Therefore, the dynamic equation of the whole parallel mechanism in operational space is written as

$$\tau_u=[I_{uu}^*]\ \ddot{u}+\ u^T[P_{uuu}^*]\ \dot{u} \tag{26}$$

In eq. (25), $[I_{uu}]$ and $[P_{uuu}]$ represent the local inertia matrix and the inertia modeling array of the remaining body which are not included in the modeling of the serial subchain. Finally, using eq. (26) and the

principle of virtual work between the output vector and the active input vector, the dynamic equations of the mechanism with respect to active joint variables can be found as

$$\tau_a = [I^*_{aa}]\ \ddot{\phi}_a + \dot{\phi}_a^T [P^*_{aaa}]\ \dot{\phi}^*_a \qquad (27)$$

4.3 Analysis on the dynamic characteristics of the 3-PPSP parallel mechanism

Ma[10] proposed dynamic isotropic index defined as

$$w_{DI} = \frac{\lambda_{\min}[I^*_{au}]}{\lambda_{\max}[I^*_{au}]} \qquad (28)$$

where $[I^*_{au}]$ represents the effective inertia matrix felt at active joints to produce the acceleration along the output direction of the mechanism. Using the principle of the virtual work, the dynamic equation between output variables and the active input variables can be written as

$$\tau_a = [I^*_{au}]\ \ddot{u} + \dot{u}^T [P^*_{auu}]\ \dot{u} \qquad (29)$$

Table 2. Dynamic parameters of a parallel manipulator

link # n	m (Kg)	$P^{(j)}_{c_j}$ (m)	$\Pi^{(j)}_{jk}$ ($Kg \cdot m^2$)
1	2.61	$[-0.015\ 0\ 0.02]^T$	
2	0.32	$[-0.01\ 0\ -0.02]^T$	
3	0	$[0\ 0\ 0]^T$	$I_{xx}=I_{yy}=I_{zz}=0$ $I_{xy}=I_{xz}=I_{yz}=0$
4	0	$[0\ 0\ 0]^T$	$I_{xx}=I_{yy}=I_{zz}=0$ $I_{xy}=I_{xz}=I_{yz}=0$
5	0.16	$[0\ 0\ 0.07]^T$	$I_{xx}=I_{yy}$ $=0.00030156$ $I_{zz}=0.00000313$ $I_{xy}=I_{xz}=I_{yz}=0$
6	0.14	$[0\ 0\ -0.1]^T$	$I_{xx}=0.00003099$ $I_{yy}=0.00003826$ $I_{zz}=0.00003192$ $I_{xy}=I_{xz}=I_{yz}=0$
Top plate	1.537	$[0\ 0\ 0]^T$	$I_{xx}=I_{yy}=0.0086538$ $I_{zz}=0.01729125$ $I_{xy}=I_{xz}=I_{yz}=0$

Table 2 represents the approximated values of the link parameters of the system and in the following simulations, these values of the link parameters are used. Fig. 6a) represents the contour plot of the dynamic isotropic index of the parallel manipulator in the $x-y$ plane when the orientation of the top plate is set to $\alpha=\beta=\gamma=0^o$, $P_{xz}=0$, and $\phi_{smax}=90^o$. Fig 6b) shows the contour plot of the dynamic isotropic index of the mechanism in the $\alpha-\beta$ plane when $P_{cz}=R$, $P_{cy}=P_{cz}=0$, $\gamma=0^o$ and $\phi_{smax}=90^o$. It can be confirmed from these plots that dynamic isotropic characteristics is more or less uniform throughout its workspace. There is a region around the boundary region of the workspace where the dynamic isotropic characteristics change rapidly. However, in real system, the hardware limitations such as limited joint angles and stroke length exclude this region from the workspace of the mechanism. Therefore, it can be contended that this mechanism has an excellent dynamic characteristics within its whole workspaces.

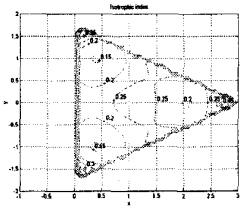

(a) $\alpha=\beta=\gamma=0^o$, $P_{xz}=0$ and $\phi_{smax}=90^o$

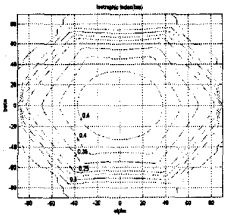

(b) $P_{cz}=R$, $P_{cy}=P_{cz}=0$, $\gamma=0^o$ and $\phi_{smax}=90^o$

Fig. 6 Contour Plots of Dynamic Isotropic Index

5. Implementation of the parallel mechanism

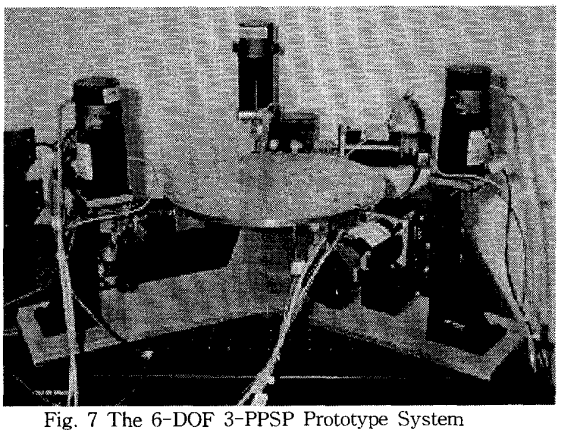

Fig. 7 The 6-DOF 3-PPSP Prototype System

5.1 System description

To test the performance of the 3-PPSP type parallel mechanism, a prototype of the mechanism shown in Fig. 7 is implemented. The implemented system hardware consists of a top plate and a base plate, 3 passive joints and 6 active prismatic joints, 6 DC servo-motors and servo-amplifiers, AD converter with 32 channels, DA converters with 12 channels, DSP control boards and a PC-586. Servo controller used in

this system is a DSP based digital control system and its sampling rate is 2kHz. As feedback position sensors, six rotary encoders and six limit sensors restricting the motion of the active prismatic actuators (i.e., its maximum stroke length is limited as $12mm$) are employed.

5.2 Experiments on movement of the prototype parallel manipulator

The desired trajectory is selected: it starts from the origin of the reference frame and follows a spiral path to the radius and then to a circular path of radius of $2.0mm$ with its center at the z axis in the $x-z$ plane without changing its output orientation as given below with a frequency of 0.5 Hz : Fig. 8a) shows the plots from the trajectory following experiments of the prototype mechanism for the given trajectory.

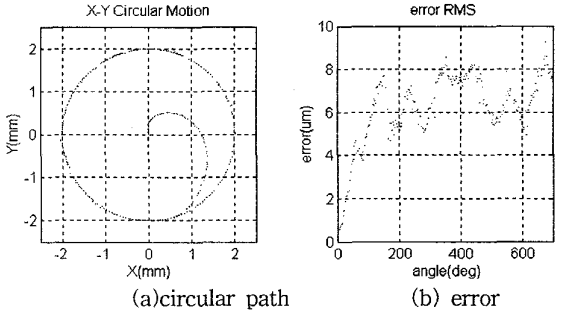

(a)circular path (b) error

Fig. 8 Experimental Results: circle motion in the $x-y$ plane

In this experiment, the joint position servo-controller (PID control) provided by the DSP control boards is directly applied to the system. It is observed that the position servo-controlled prototype system shows relatively good trajectory following capability. In Fig. 8b), the output position errors are computed by comparing the output position computed analytically from the forward position analysis using the measured joint angular displacement data with the given trajectory. As can be seen in Fig. 8 b), the system follows the given circular path with an error variation bounds of $7\mu m$. Lastly, noting the manipulator has closed-form forward/reverse position solutions[5], its computatonal burden is significantly reduced. Thus, it is expected that more advanced controller requiring heavy computational burden can be applied to the system in real time, further to enhance the performane of the system. Currently, this process is under study.

6. Conclusion

In previous study, the 3-PPSP parallel mechanism is proposed and it is shown that the mechanism has a closed form of forward/reverse position solution and a relatively large workspace[5]. In this study, the kinematic/dynamic analysis of the 3-PPSP parallel mechanism is performed and its kinematic/dynamic isotropic characteristics is investigated and showed that the mechanism has a uniform kinematic/dynamic isotropic characteristics throughout workspace. From these results, it is proven that the 3-PPSP mechanism has an excellent geometric, kinematic and dynamic characteristics. In addition, a prototype system is built and a few simple peformance tests are conducted, applying a simple position servo controller to the system. From the experiments, it is shown that the mechanism has a good trajectory following performance. Particularly, it is expected that when more advanced controller is applied to the system, much higher precision performance of the system is achieved. Conclusively, it can be contended from this study that the mechanism has a very high precision capability and can be effectively employed in tasks requiring real-time operation.

References

[1] Reboulet, C., Berthomieu, T., 1991, "Dynamic Models of a Six Degree of Freedom Parallel Manipulators," Proc. of IEEE/RSJ Int'l Conf. on Intelligent Robots and Systems, pp. 1151-1157.

[2] Thomas, M. and Tesar, D., "Dynamic Modeling of Serial Manipulator Arms," Trans. ASME 1982, Sep. Vol.104, pp 218-227.

[3] R.A. Freeman, and D. Tesar, "Dynamic Modeling of Serial and Parallel Mechanisms/Robotic Systems, Part I-Methodology, Part II-Applications", Proc. 20th ASME Biennial Mechanisms Conf. Orlando, FL, Trends and Development in Mechanisms, Machines, and Robotics, 1988, DE-Vol. 15-3, pp.7-27.

[4] M. Sklar & D. Tesar, "Dynamic Analysis of Hybrid Serial Manipulator Systems Containing Parallel Modules," ASME Trans. Journal of Mech. Trans. and Automation in Design, 1984.

[5] Y.K. Byun and H.S. Cho, "Analysis of a Novel Six-Degree-of-Freedom 3-PPSP Parallel Manipulator," Journal of Robotics Research, Vol.16, No.6 Dec., 1997, Vol 16 Iss:6p pp. 859-872.

[6] W.K. Kim, Y.K.Byun, H.S.Cho, "Closed Form Solution of Forward Position Analysis for a 6 DOF 3-PPSP Parallel Mechanism of General Geometry," '98 IEEE Conf. Robotics and Automation.